Curcumin inhibits the cancer-associated fibroblast-derived chemoresistance of gastric cancer through the suppression of the JAK/STAT3 signaling pathway

IN-HYE HAM[1,2*], LEI WANG[3,4*], DAGYEONG LEE[1,5], JONGSU WOO[1,5], TAE HOON KIM[1,5], HYE YOUNG JEONG[6], HYE JEONG OH[1], KYEONG SOOK CHOI[7], TAE-MIN KIM[6] and HOON HUR[1,2,5]

[1]Department of Surgery, Ajou University School of Medicine; [2]Inflamm-Aging Translational Research Center, Ajou University School of Medicine, Suwon, Gyeonggi-do 16499, Republic of Korea; [3]Department of Pathology, Fudan University Shanghai Cancer Center; [4]Department of Oncology, Shanghai Medical College, Fudan University, Shanghai 200032, P.R. China; [5]Department of Biomedical Sciences, Graduate School of Ajou University, Suwon, Gyeonggi-do 16499; [6]Department of Medical Informatics, College of Medicine, The Catholic University of Korea, Seoul 16591; [7]Department of Biochemistry and Molecular Biology, Ajou University School of Medicine, Suwon, Gyeonggi-do 16499, Republic of Korea

Received February 3, 2022; Accepted May 4, 2022

DOI: 10.3892/ijo.2022.5375

Abstract. The present study aimed to investigate whether the Janus-activated kinase (JAK)/signal transducer and activator of transcription 3 (STAT3) signaling pathway is a critical mechanism underlying the cancer-associated fibroblast (CAF)-induced chemoresistance of gastric cancer (GC). In addition, the present study tried to suggest a natural product to compromise the effects of CAF on the chemoresistance of GC. The results of cell proliferation assay revealed that the conditioned medium (CM) collected from CAFs further increased resistance to 5-fluorouracil (5-FU) in GC cell lines. Secretome analysis revealed that the levels of several secreted proteins, including C-C motif chemokine ligand 2, C-X-C motif chemokine ligand 1, interleukin (IL)-6 and IL-8, were increased in the CM from CAFs co-cultured with cancer cells compared to CM from cancer cells. Western blot analysis revealed that CAFs activated the JAK/STAT3 signaling pathway in cancer cells. The experimental models revealed that curcumin abrogated the CAF-mediated activation of the JAK/STAT3 signaling pathway in GC cells. *In vivo* data revealed the synergistic effects of curcumin with 5-FU treatment in xenograft GC tumors. These data strongly suggest that the suppression of the JAK/STAT3 signaling pathway counteracts the CAF-induced chemoresistance of GC cells. It is suggested that curcumin may be a suitable natural product which may be used to overcome chemoresistance by inhibiting the CAF-induced activation of the JAK/STAT3 signaling pathway in GC.

Correspondence to: Professor In-Hye Ham or Professor Hoon Hur, Department of Surgery, Ajou University School of Medicine, Room 212, 164 Worldcup-ro, Yeongtong-gu, Suwon, Gyeonggi-do 16499, Republic of Korea
E-mail: atoropos86@naver.com
E-mail: hhcmc75@ajou.ac.kr

*Contributed equally

Abbreviations: 5-FU, 5-fluorouracil; CAF, cancer-associated fibroblast; CCL2, C-C motif chemokine ligand 2; CM, conditioned medium; GC, gastric cancer; H&E, hematoxylin and eosin; IHC, immunohistochemistry; IL-6, interleukin-6; IL-8, interleukin-8; JAK, Janus-activated kinase; KEGG, Kyoto Encyclopedia of Genes and Genomes; STAT3, signal transducer and activator of transcription 3

Key words: gastric cancer, cancer-associated fibroblast, curcumin, chemoresistance, tumor microenvironment

Introduction

Gastric cancer (GC) is one of the most common malignant tumors worldwide (1). Although the current mortality rate of GC has decreased, unresectable GC remains intractable (2). Guidelines for GC indicate that the primary treatment option for advanced-stage GC is palliative chemotherapy (3,4); however, the majority of patients develop resistance, as the mean survival rate for these patients is ~1 year. Several agents targeting the molecules expressed in GC cells have been used to enhance the therapeutic efficacy of chemotherapy in GC. However, apart from HER2 or VEGFR2 inhibitors, the majority of drugs did do not lead to an improved survival. Comprehensive molecular analysis has revealed that a high proportion of non-cancerous stroma within the primary tumor of GC leads to a poor prognosis and an unsatisfactory response to chemotherapy (5,6).

Cancer-associated fibroblasts (CAFs) are one of the major components of GC stromal areas. Previous studies have demonstrated that CAFs enhance the resistance of

GC to chemotherapy (7,8). However, the exact mechanisms involved in CAF-induced resistance to therapy have not yet been described, and inhibitors to suppress the effect of CAF have not yet been applied in clinical settings, at least to the best of our knowledge. CAFs can produce various cytokines and growth factors, which can activate intracellular signaling pathways in cancer cells (9,10). It has been described that the Janus-activated kinase (JAK)/signal transducer and activator of transcription 3 (STAT3) axis may be the primary signal transduction pathway activated by CAF-produced cytokines and chemokines (11). Moreover, it plays a crucial role in enhancing resistance to cancer therapy (12). Taken together, the JAK/STAT3 pathway may be considered a promising target which may be used to combat the CAF-induced resistance of GC to chemotherapy.

The JAK/STAT3 signaling pathway is an attractive target for cancer treatment as it can promote the proliferation, survival and migration of cancer cells (13). Although the US Food and Drug Administration (FDA) approved the JAK1/2 inhibitor, ruxolitinib, for hematopoietic neoplasms, the benefit of JAK- or STAT3-specific inhibitors has not been reported in clinical trials for solid malignancies (14). Moreover, the JAK/SATA3 pathway has a variety of biological functions in normal cells and tissues; therefore, blocking this pathway requires a proper appreciation of the possible side-effects associated with its inhibition (12,15,16).

Recent studies have reported that phytochemicals, such as flavonoids or polyphenols in medicinal and edible plants have antioxidant, anti-inflammatory and anticancer properties. Among the numerous phytochemicals, curcumin (diferuloylmethane), a polyphenol compound derived from the roots of *Curcuma longa*, is a biologically active compound of the Indian spice, turmeric. This compound has been shown to possess biological activities, such as antioxidant, antimicrobial, anti-inflammatory and anticancer activities (17-20). In a previous study, curcumin was found to exert a potent antitumor effect in human uterine leiomyosarcoma SKN cells via the inhibition of the activity of the AKT/mTOR pathway (21). Furthermore, another study reported that curcumin blocked the initial carcinogenic process in colorectal cancer animal models induced by azoxymethane (22).

In a previous study, curcumin was shown to inhibit the STAT3 signaling pathway by binding to the JAK activation loop in a time-and concentration-dependent manner (23). However, the suppressive effects of curcumin on the development of chemotherapeutic resistance in GC have not yet been evaluated, at least to the best of our knowledge. Thus, the present study aimed to determine whether curcumin can effectively suppress the CAF-mediated resistance to 5-fluorouracil (5-FU) in GC cells.

Materials and methods

Cells and cell culture. The GC cell lines, MKN1 (KCLB no. 80101), MKN74 (KCLB no. 80104) and SNU668, (KCLB no. 00668) were purchased from the Korean Cell Line Bank. The cells were cultured in RPMI-1640 medium (HyClone; Cytiva) supplemented with 10% fetal bovine serum (FBS; HyClone; Cytiva), 1% penicillin-streptomycin (Gibco; Thermo Fisher Scientific, Inc.) and 1% amphotericin B (SEARCH BIO Inc.). The cells were incubated at 37˚C in a humidified atmosphere containing 5% CO_2. CAFs were isolated from fresh GC patient specimens as described in a previous study by the authors (24). For co-cultures, CAFs were seeded into the upper chambers of 6-well Transwells and GC cell lines were seeded into the bottom of six-well tissue culture dishes. DMEM/high glucose medium (HyClone; Cytiva; supplemented with 5% FBS) was added to both the upper and bottom chambers, allowing interaction between the two cell types.

Reagents. The STAT3 inhibitor (WP1066; cat. no. 573097) and 5-FU (cat. no. F6627) were purchased from MilliporeSigma. Recombinant human C-C motif chemokine ligand 2 (CCL2; cat. no. 279-MC-050), C-X-C motif chemokine ligand (CXCL)1 (cat. no. 275-GR-010) and CXCL8 (cat. no. 208-IL-050) were purchased from R&D Systems, Inc., and recombinant human interleukin (IL)-6 (cat. no. PHC0064) was purchased from Gibco; Thermo Fisher Scientific, Inc.

Western blot analysis. Cells were washed with phosphate-buffered saline (PBS) and lysed in boiling sodium dodecyl sulfate-polyacrylamide gel electrophoresis (SDS-PAGE) sample buffer [62.5 mM Tris (pH 6.8), 1% SDS, 10% glycerol and 5% β-mercaptoethanol]. The lysates were scraped on a plate with a pipette and boiled for 5 min at 100˚C. Protein concentrations were determined using the reducing agent compatible/detergent compatible RC/DC protein assay (Bio-Rad Laboratories, Inc.). Equal amounts (30 μg) of protein from each sample were resolved by SDS-PAGE and transferred onto a polyvinylidene difluoride membrane (MilliporeSigma). The immunoblots were blocked by incubation in 5% skim milk, 25 mM Tris (hydroxymethyl) aminomethane-HCl (pH 8.0), 150 mM NaCl, and 0.1% Tween®-20 for 1 h at 25˚C. The membranes were incubated overnight at 4˚C with the following primary antibodies: Anti-STAT3 (1:1,000 dilution; cat. no. 9139), anti-phosphorylated (p-) STAT3 (1:1,000; cat. no. 9145), anti-AKT (1:1,000; cat. no. 9272), anti-p-AKT (1:1,000; cat. no. 4060), anti-mTOR (1:1,000; cat. no. 2972), anti-p-mTOR (1:1,000; cat. no. 2971S), anti-cleaved PARP (1:1,000; cat. no. 9542; Cell Signaling Technology), anti-cleaved caspase-3 (1:1,000; cat. no. 9664) (all from Cell Signaling Technology, Inc.), anti-Bcl-2 (1:1,000; cat. no. sc-509; Santa Cruz Biotechnology, Inc.), anti-survivin (1:500; cat. no. ADI-AAP-275; Enzo Life Sciences, Inc.) anti-β-actin (1:5,000; cat. no. sc-47778; Santa Cruz Biotechnology, Inc.). The membranes were then washed three times with Tris-buffered saline with Tween-20 (TBST), followed by their corresponding horseradish peroxidase-conjugated secondary antibodies (1:5,000; cat. no. 115-545-146; Jackson ImmunoResearch Laboratories, Inc.) for 1 h at room temperature. Protein detection was performed using an enhanced chemiluminescence kit (AbClon, Inc.). The pixel volumes were evaluated using ImageJ software (version 1.52; National Institutes of Health), and the results were normalized to the corresponding blots.

Cell viability assay. The cells were seeded at $1x10^4$ cells per well in 96-well plates, and cell proliferation was measured using a highly sensitive water-soluble tetrazolium salt-based viability assay kit (DoGen Bio). After seeding the cells, 10 μl

EZ-Cytox solution were added per well, and the cells were incubated for 1 h at 37˚C. The absorbance was measured at 450 nm using a Tecan microplate reader (Infinite F50; Tecan Group, Ltd.). All experiments were performed in triplicate. To evaluate the effects of curcumin on cell viability, the cells were treated with various concentrations (0.2, 1.0, 5.0, 25, 125, 625 and 3,125 μM) of 5-FU for 72 h. The To IC_{50} values were calculated as follows: The inhibitor concentration against the percent activity is plotted [(I)-activity % graph]. Using the linear (y=mx + n) or parabolic (y=ax2 + bx + c) equation on this graph for y=50 value x point yields the IC_{50} value.

Secretome and transcriptome analysis. Secretome analysis was performed using the Proteome Profiler Human Cytokine Array kit (R&D Systems Inc.) to identify upregulated secretory factors in the culture supernatants of MKN1, MKN74 and SNU668 cells co-cultured with CAFs as compared with MKN1, MKN74, and SNU668 cells cultured without CAFs. Conditioned medium (CM) from the MKN1, MKN74, and SNU668 cell cultures was collected after 48 h in serum-free medium and incubated with arrays containing 36 human cytokine-specific antibodies at 4˚C for 24 h. After the membranes were treated with a luminescence reagent, X-ray films were developed to identify the pixel volume of the spots related to the quantity of each secreted protein. The pixel volumes were evaluated using ImageJ software (version 1.52; National Institutes of Health), and the results were normalized to the corresponding spots. Using RNeasy (Qiagen, Inc.), RNA was extracted from the MKN1, MKN74 and SNU668 cells cultured alone or together with CAFs. The RNA quality was assessed using a 2100 Bioanalyzer (Agilent Technologies, Inc.) and cDNA was synthesized using the GeneChip WT (Whole Transcript) Amplification kit (Thermo Fisher Scientific, Inc.). Labeled target DNA (~5.5 μg) was hybridized to Affymetrix GeneChip Human Gene 2.0 ST Arrays (Thermo Fisher Scientific, Inc.). Array data processing and analysis were performed using Affymetrix GeneChip Command Console Software (6.0+ version; Thermo Fisher Scientific, Inc.). Gene set enrichment analysis (GSEA) was used to identify upregulated pathways in MKN74 and SNU668 cells co-cultured with CAFs relative to MKN74 and SNU668 cells alone. Pathway categories were obtained from the Molecular Signatures Database (MSigDB, https://software.broadinstitute.org). The cut-off value for statistical significance used in GSEA was a false discovery rate (FDR) of 25%. To reduce the likelihood of false-positive results, the present study used an FDR value of 5% as the cut-off level for enriched gene sets.

Patient samples. Of the patients diagnosed with GC who were treated with neoadjuvant chemotherapy/chemoradiotherapy following surgery at the Shanghai Cancer Center, Shanghai, China from July, 2019 to October, 2020, surgically resected paraffin-embedded tissues from 50 patients were collected. Normal tissue collected from adjacent tumor area in patients. The use of these specimens was approved by the Institutional Review Board of Shanghai Cancer Center (IRB no. 050432-4-1911D). Informed consent was obtained from all the participants. The combined regimens based on 5-FU were administered for neoadjuvant chemotherapy from two to six cycles, and 7 patients were additionally treated with radiation at 4,500 cGy. Following chemotherapy or chemoradiation therapy, all patients were curatively resected by total or subtotal gastrectomy with proper lymph node dissection.

All hematoxylin and eosin (H&E)-stained sections were reviewed by an experienced pathologist (LW) to confirm the GC cancer proportion and to be assigned a grade of responsiveness to chemotherapy in the primary GC tissues according to the grading system suggested by the national comprehensive cancer network (25).

Immunohistochemistry (IHC). Formalin-fixed paraffin-embedded xenograft and primary GC tumors were sectioned, affixed onto microscopic slides, deparaffinized with xylene, hydrated using a diluted alcohol series, and immersed in 0.3% H_2O_2 in methanol to quench endogenous peroxidase activity. The sections were treated with citrate buffer (10 mM, pH 6.0) for antigen retrieval. To reduce non-specific staining, each section was treated with 20% aqua block (Abcam) in TBST for 30 min. The sections were incubated overnight at 4˚C with the primary rabbit monoclonal anti-cleaved caspase-3 antibody (1:100; cat. no. 9664, Cell Signaling Technology, Inc.) for xenograft tumors and the primary rabbit monoclonal anti-p-STAT3 antibody (1:100; cat. no. 9145, Cell Signaling Technology, Inc.) for human GC primary tumors in antibody diluent solution (GBI Labs). The following day, the sections were incubated with polyclonal anti-rabbit secondary antibody (1:100; cat. no. AbC-5003; AbClon, Inc.) for 60 min at room temperature. The chromogen used was 3,3'-diaminobenzidine (Thermo Fisher Scientific, Inc.), and the sections were counterstained with Harris hematoxylin (cat. no. S3309, Dako; Agilent Technologies, Inc.) at room temperature for 5 min. For cleaved caspase-3 immunohistochemical analysis of the harvested tumor tissue, the images were captured using an Olympus BX53 microscope with an Olympus DP73 camera (Olympus Corporation) at x200 magnification. In the images, the areas of entire tumors and brown-stained lesions were quantified by densitometry using ImageJ software (version 1.52; National Institutes of Health). The percentage of apoptotic cells was calculated as the ratio of stained area to the total area. Differences in apoptotic marker expression among the treatment groups were analyzed using the Mann-Whitney U test.

Analysis of gene expression dataset for GC. To investigate the association of STAT3-related genes and the tumor stroma with outcomes of patients with GC, GC mRNA profile data were downloaded from the publicly available GEO database (GSE62254) with 300 GC patient samples and clinical information and Kyoto Encyclopedia of Genes and Genomes (KEGG) pathway analyzed using GSEA methods. The GSE62254 dataset was generated based on the GPL570 platform (Affymetrix Human Genome U133 Plus 2.0). To infer the proportion of stromal fibroblasts in GC tissues, the Estimation of Stromal and Immune cells in MAliganant tumor tissues (ESTIMATE) algorithm on the transcriptome data was used. In addition, to annotate gene sets related to the STAT3 signaling pathway, MSigDB we used, and the STAT3 pathway was one of the C2 gene sets representing canonical pathways from pathway resources. A total of eight genes (*MAPK3*, *TYK2*, *JAK1*, *MTOR*, *MAP1*, *STAT3*, *JAK3* and *JAK2*) were included in the STAT3 pathway, and patients were classified into the

high and low STAT3 pathway expression groups using the median expression of the eight genes as the cut-off value. The correlations of the STAT3 pathway gene set with the stromal score and several cytokine- or chemokine-related genes were evaluated using Pearson's correlation analysis. Kaplan-Meier analysis and log-rank tests were used to investigate the survival difference between the high and low mean expression of actin alpha 2 (*ACTA2*), a marker of activated fibroblasts, and *STAT3* genes.

Flow cytometric analysis. The MKN1, MKN74 and SNU668 cells were seeded in a six-well plate and treated with 5-FU (100 μM), CAF co-culture and curcumin (20 μM) for 72 h. The cells were stained with fluorescein isothiocyanate (FITC)-conjugated Annexin V and propidium iodide (PI). FITC Annexin V and PI double-positive cells were detected using a FACSCanto II flow cytometer (BD Biosciences).

Animal model experiment. Animal care and handling procedures were performed in accordance with the Ajou University School of Medicine Institutional Animal Care and Use Committee guidelines, and all animal experiments were approved by the Animal Research Committee of the institution. The animal model was established using six- to eight-week-old male athymic nude mice (Orient Bio, Inc.) weighing 16-18 g. For the experiments, four 4 groups of mice were used with 6 mice in each group. The mice in all groups were intraperitoneally injected with $1x10^6$ SNU668 cells with $1x10^6$ CAFs. The groups were as follows: Group 1, untreated mice; group 2, mice treated with curcumin alone; group 3, mice treated with 5-FU alone; and group 4, mice treated 5-FU with curcumin. To establish xenograft tumors, the cells were suspended in 50 μl Matrigel mixed with PBS. In total, $1x10^6$ tumor cells (SNU668) with $5x10^5$ fibroblasts were subcutaneously implanted into the flanks of BALB/c-nu nude mice (Orient Bio, Inc.). To investigate the effects of 5-FU and curcumin on tumor formation in the mice, at 7 or 10 days following cell transplantation, the mice were treated intraperitoneally with 5-FU (25 μg/g body weight) and curcumin (100 μg/g body weight) three times a week for 3 weeks. Tumor volume and body weight were monitored throughout the study period. In all experiments, tumor dimensions were measured using calipers, and the tumor volume was calculated using the following formula: Tumor volume (mm^3)=(a x b^2)/2, where a=length in mm, and b=width in mm. The method of euthanasia used for the mice was CO_2 asphyxiation followed by cervical dislocation (CO_2 was introduced into the chamber at a rate of 30-70% of the chamber volume per min to minimize distress). After euthanizing the mice, all tumors were harvested for tumor weight measurement and IHC staining.

Statistical analysis. All experiments were performed independently in triplicate. The results are presented as the mean ± standard error (SE). To compare means of continuous variables between the two groups, datasets were analyzed using an unpaired or paired t-test for normally distributed data or a Mann-Whitney U test or Wilcoxon test for non-normal data. A one-way analysis of variance (ANOVA), followed by Tukey's post hoc test, was used to compare means across three or more groups. The Chi-squared test was used to determine whether there was an association between two or more categorical variables. Statistical analyses were performed using IBM SPSS statistics (version 21 for Mac OS X; IBM, Inc.) and GraphPad Prism (version 6.0, for Mac OS X; GraphPad Software, Inc.) software. The bioinformatics data using the public dataset were analyzed using the R package. Values of $P<0.05$, $P<0.01$ or $P<0.001$ were considered to indicate statistically significant or highly statistically significant differences, respectively.

Results

CAFs induce chemoresistance to 5-FU in GC cell lines. To initially evaluate the paracrine effects of CAFs on the resistance of GC cell lines to chemotherapy, first, CM was isolated from CAFs (CAF-CM), which was added to the MKN1, MKN74 and SNU668 cells treated with 5-FU. The MKN1, MKN74 and SNU668 cells stimulated with CAF-CM exhibited a greater resistance (higher IC_{50}) to 5-FU than those cultured in normal medium, as revealed by a cell viability test (Fig. 1A). In addition, a Transwell co-culture system was used to investigate the CAF-induced changes in apoptotic markers, including the expression of PARP and caspase-3. It was found that co-culture with CAFs markedly decreased the expression of cleaved PARP and caspase-3 in the 5-FU-treated MKN1, MKN74 and SNU668 cells (Fig. 1B). In addition, it was found that the 5-FU-induced apoptotic morphologies, including cellular shrinkage and the formation of apoptotic bodies, as well as the reduction in live (attached) cell numbers were markedly attenuated in the cancer cells co-cultured with CAFs. When treated with 5-FU, while the majority of the GC cells were killed or scattered, the CAF-co-cultured GC cells displayed a normal morphology (Fig. 1C). These results suggest that CAFs confer the resistance to 5-FU of GC cell lines through the suppression of apoptosis.

CAFs activate the JAK2/STAT3 signal transduction pathway in GC cell lines. To identify CAF-specific secreted molecules and CAF-induced gene expression in GC cells, secretome analysis for CM and transcriptome analysis of GC cells co-cultured with CAFs were performed. It was hypothesized that increased proteins in the CM of GC cells co-cultured with CAFs, compared to the CM of GC cells cultured without CAFs, would be the main ligands to stimulate GC cells. Thus, the levels of secreted proteins in CM between GC and GC co-culture with CAFs were compared (Fig. 2A). In most pairs, the intensity of CCL2, CXCL1, IL-6 and IL-8 in the CM from GC cells co-cultured with CAFs was higher than that in the GC cells not cultured with CAFs (Fig. 2A). Subsequently, under the same conditions as the secretome analysis, transcriptome analysis was performed using mRNA extracted from the harvested GC cells. The results revealed that mRNA extracted through GSEA was positively associated with IL-6/JAK/STAT3 signaling (Fig. 2A; MKN-74 cell enrichment score, 1.83; nominal $P<0.001$, FDR $Q=0.001$, FWER $P=0.006$; SNU668 cell enrichment score, 1.45; nominal $P<0.01$, FDR $Q=0.01$, FWER $P=0.145$).

The genes encoding the secreted proteins were functionally annotated according to the KEGG pathway map (https://www.genome.jp/kegg/). *CCL2*, *CXCL1*, *IL-6* and *CXCL8* are involved in cytokine-chemokine receptor interactions and

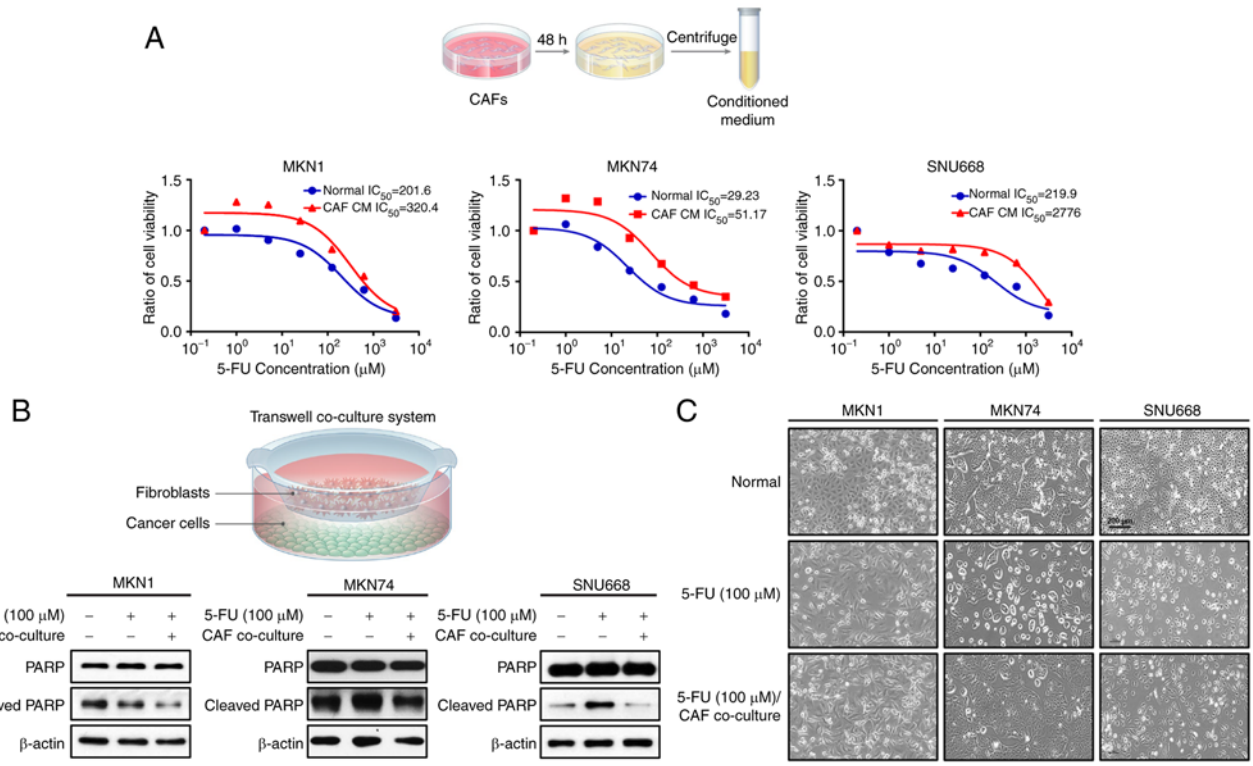

Figure 1. CAF-induced resistance to 5-FU in GC cells. (A) GC cells were co-cultured with fibroblast culture-conditioned media and treated with 5-FU and the IC_{50} value was determined. (B) Western blot analysis showing the expression levels of the indicated proteins following 5-FU treatment with and without co-culture with CAFs in various GC cell lines. (C) Representative photomicrograph demonstrating the morphological changes in GC cells following 5-FU treatment for 72 h co-culture with or without CAFs. 5-FU, 5-fluorouracil; CAF, cancer-associated fibroblast; GC, gastric cancer. Scale bar, 200 μm.

chemokine signaling pathways, including the JAK/STAT3 signaling pathway (Fig. 2B).

In addition, using western blot analysis, it was confirmed that JAK2, STAT3, Bcl-2 and survivin were associated with the JAK/STAT3 signal transduction pathway. Likewise, the GC cell lines co-cultured with CAFs exhibited increased phosphorylation levels of JAK2 (STAT3 upstream protein), Bcl-2 and survivin (STAT3 downstream proteins) (Fig. 2C). To confirm the CAF-induced chemoresistance of GC cell lines treated with 5-FU, western blot analysis was performed for the GC cell lines co-cultured with CAFs. The GC cell lines co-cultured with co-culture CAFs exhibited increased p-STAT3 levels when treated with 5-FU. However, another pathway was not altered when the cells were co-cultured with CAFs (Fig. 2D). Through this process, it was expected that the co-culture of GC cells and CAFs would affect the intercellular signaling pathway in GC cells, particularly the JAK2/STAT3 signaling pathway.

Upregulation of p-STAT3 is associated with the non-responsiveness of human primary GC tumors treated with neoadjuvant therapy. Primary GC tumors, which were harvested from the Shanghai Cancer Center cohort treated with neoadjuvant chemotherapy, were divided into the response (grade I/II) and non-response (grade III/IV) groups. These groups were selected according to the pathological responsiveness of the surgical specimens following neoadjuvant chemotherapy (Fig. 3A), and IHC for p-STAT3 was measured from 0 to 80% according to the proportion of cells with positive staining (Fig. 3B, images). The mean proportion of p-STAT3 expression did not markedly differ between the two groups. However, when the expression of p-STAT3 was determined to be positive when the proportion of positive cells was ≥3%, the positive expression of p-STAT3 was significantly associated with a high proportion of poor responsiveness (P=0.048; Fig. 3B, table).

The high expression of the STAT3 pathway gene set is significantly associated with a high stromal gene score and a poor prognosis of patients with GC. A cohort containing 299 GC patients with available transcriptome data (GSE62254) and clinical information from a previously published report was analyzed (26). All patients included in this dataset were diagnosed with advanced GC with T2 and greater depth of invasion, and 90.3% were stage II or higher (Fig. 3C). According to the ESTIMATE algorithm, the infiltration of stromal cells into tumor tissue was estimated. A 'stromal score' was generated to reflect the presence of fibrotic stromal cells in tumor tissues using the 141 genes proposed (27). In the same dataset, a 'STAT3_PATHWAY_GENES' was calculated using eight genes generated from the MSigDB database. To investigate the correlation between the 'stromal score' and 'STAT3_PATHWAY_GENES', Pearson's correlation analysis was used and a positive correlation was revealed (r=0.29, P<0.001). In addition, the correlation between the genes encoding the suggested proteins and 'STAT3_PATHWAY_GENES' was evaluated. The expression of *CCL2*, *CXCL1*, *IL-6* and *CXCL8* positively correlated with 'STAT3_PATHWAY_GENES' in the GSE62254 dataset (Fig. 3D).

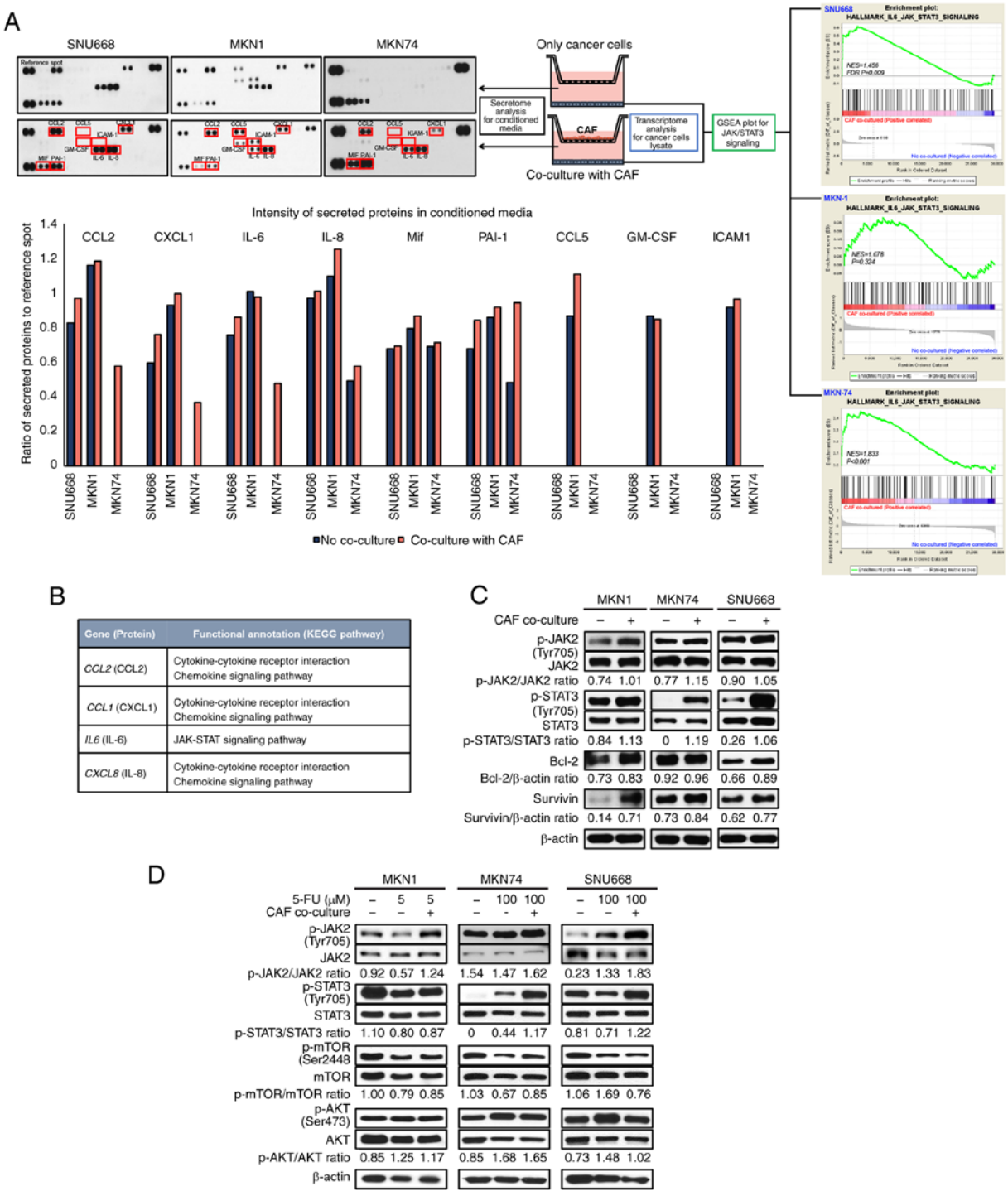

Figure 2. Identification of the JAK2/STAT3 axis as a specific communicator between CAFs and GC cells. (A) Schematic diagram of secretome analysis of conditioned media and transcriptome and western blot analysis for MKN1 cells, MKN74 cells and SNU668 cells. *IL-6*, *IL-8* and *CCL2* were secreted at higher levels in co-cultured with CAFs relative to MKN74 cells and SNU668 cells cultured alone. These factors were all associated with the JAK/STAT3 signal transduction pathway. Gene set enrichment analysis revealed that the IL-6/JAK/STAT3 signaling-related genes were enriched in MKN74 cells and SNU668 cells co-cultured with CAFs (MKN-74 cell enrichment score, 1.83, nominal P<0.001, FDR Q=0.001, FWER P=0.006; SNU668 cell enrichment score, 1.456; nominal P<0.01, FDR Q=0.01, FWER P=0.145). (B) KEGG pathway analysis expressed increased genes between no co-culture and co-culture with CAFs in MKN1 cells, MKN74 cells and SNU668 cells. (C) Western blot analysis showing the expression levels of the indicated proteins after co-culture with CAFs in MKN1 cells, MKN74 cells and SNU668 cells. (D) Western blot analysis showing the expression levels of the indicated proteins following 5-FU treatment with or without co-culture with CAFs in MKN1 cells, MKN74 cells and SNU668 cells. 5-FU, 5-fluorouracil; CAF, cancer-associated fibroblast; GC, gastric cancer; CCL2, C-C motif chemokine ligand 2; KEGG, Kyoto Encyclopedia of Gene and Genomes; IL-6, interleukin-6; IL-8, interleukin-8; JAK, Janus-activated kinase; STAT3, signal transducer and activator of transcription 3.

In the same cohort, the present study also aimed to identify the prognostic role of the simultaneous expression of *ACTA2*, a marker of fibroblasts, and *STAT3* genes in the outcomes of GC patients using the Kaplan-Meier curve with the log-rank test. Patients with GC with high mean expression of *ACTA2* and *STAT3* exhibited a significantly worse prognosis compared

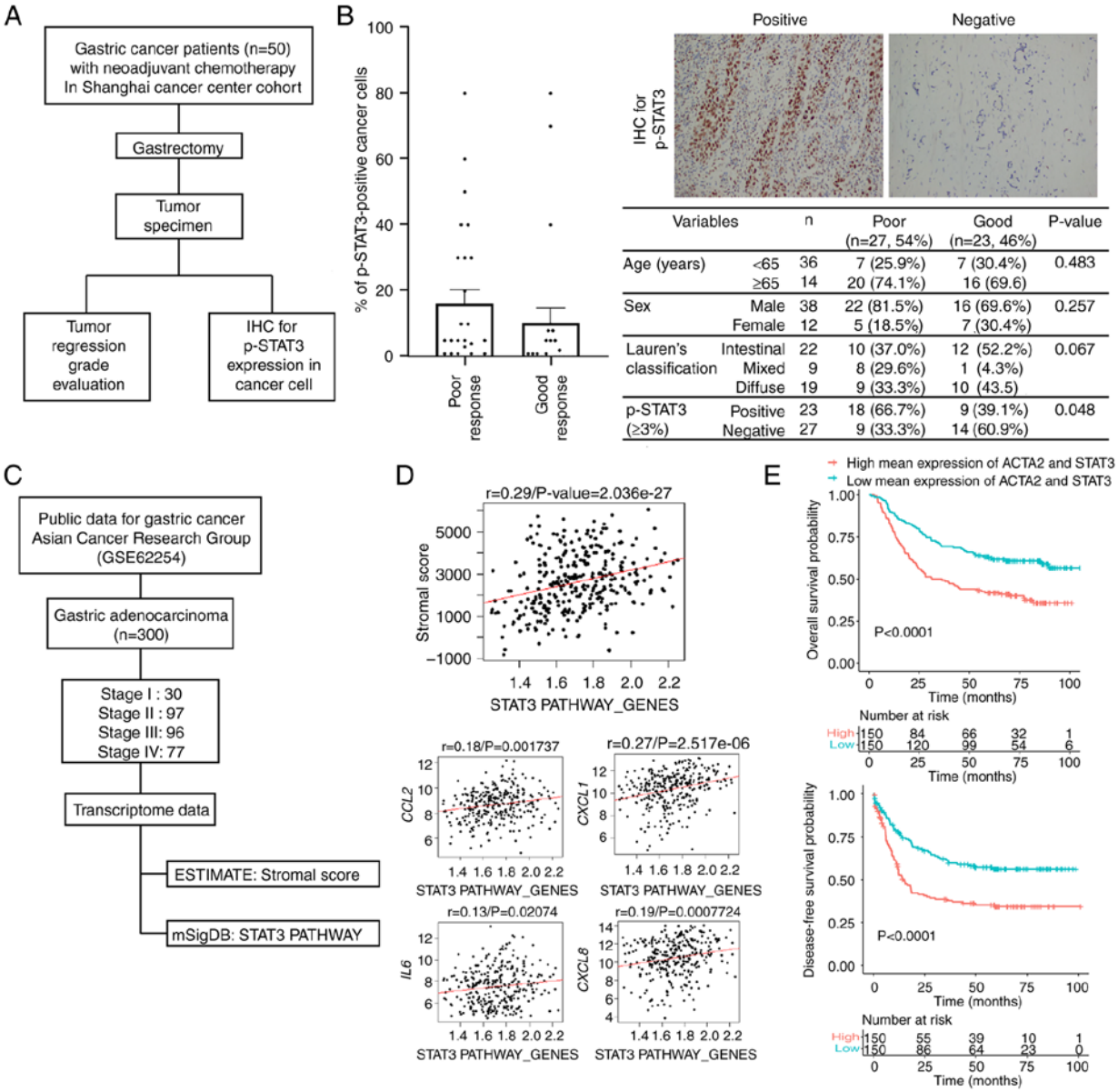

Figure 3. Expression of STAT3 and p-STAT3 in human primary GC tissues. (A) Flow diagram presenting the study scheme using human primary tumors of GC patients who were treated with neoadjuvant chemotherapy/chemoradiation following as curative resection. (B) The proportion of p-STAT3-positive cancer cells in immunohistochemistry for primary GC tumors according to the responsiveness for neoadjuvant therapy. Representative image (magnification, x200) for p-STAT staining and table showing the association between clinicopathological factors and the responsiveness to neoadjuvant therapy. These data were analyzed using the Chi-squared test. (C) Flow diagram presenting the study scheme using the public transcriptome dataset (GES62254) for human primary samples. (D) The correlation between STAT3 pathway gene set and stromal gene score, CCL2, CXCL1, IL-6, and CXCL8 expression in GSE62254 dataset. (E) Survival differences according to the expression of STAT3 pathway gene set in the GSE62254 dataset. CCL2, C-C motif chemokine ligand 2; GC, gastric cancer; IL-6, interleukin-6; STAT3, signal transducer and activator of transcription 3.

to patients with a low expression (P<0.0001) and a worse disease-free survival (P<0.0001) (Fig. 3E). These human GC data may suggest that the accumulation of a fibrotic stroma, including CAFs is significantly associated with STAT3 activation, and CAF-secreted proteins, such as CCL2 and CXCL1 enhance the STAT3 signaling pathway in GC tissues. The activation of STAT3 in the GC stroma leads to resistance to treatments, and thus this may be a good target for GC treatment.

Curcumin inactivates the CAF-induced activation of the JAK2/STAT3 signal transduction pathway in GC cell lines. It was hypothesized that CAFs may participate in the development of drug resistance through the activation of the JAK2/STAT3 pathway. Thus, the effects of curcumin on the tendency of CAFs to lead to chemoresistance and the phosphorylation of JAK2/STAT3 in GC cell lines were investigated. First, the toxicity of curcumin on cancer cells was evaluated, and the results revealed that the effects of curcumin at ≤20 μM on cell viability of GC cell lines were minimal (Fig. S1). Moreover, curcumin at <20 μM significantly decreased the CAF-induced phosphorylation of JAK/STAT3 in GC cells in a concentration-dependent manner (Fig. 4A). Curcumin also affected the expression of Bcl-2 and survivin, which are downstream of the STAT3 pathway in GC cell lines (Fig. 4A). However, curcumin treatment did not decrease the phosphorylation of

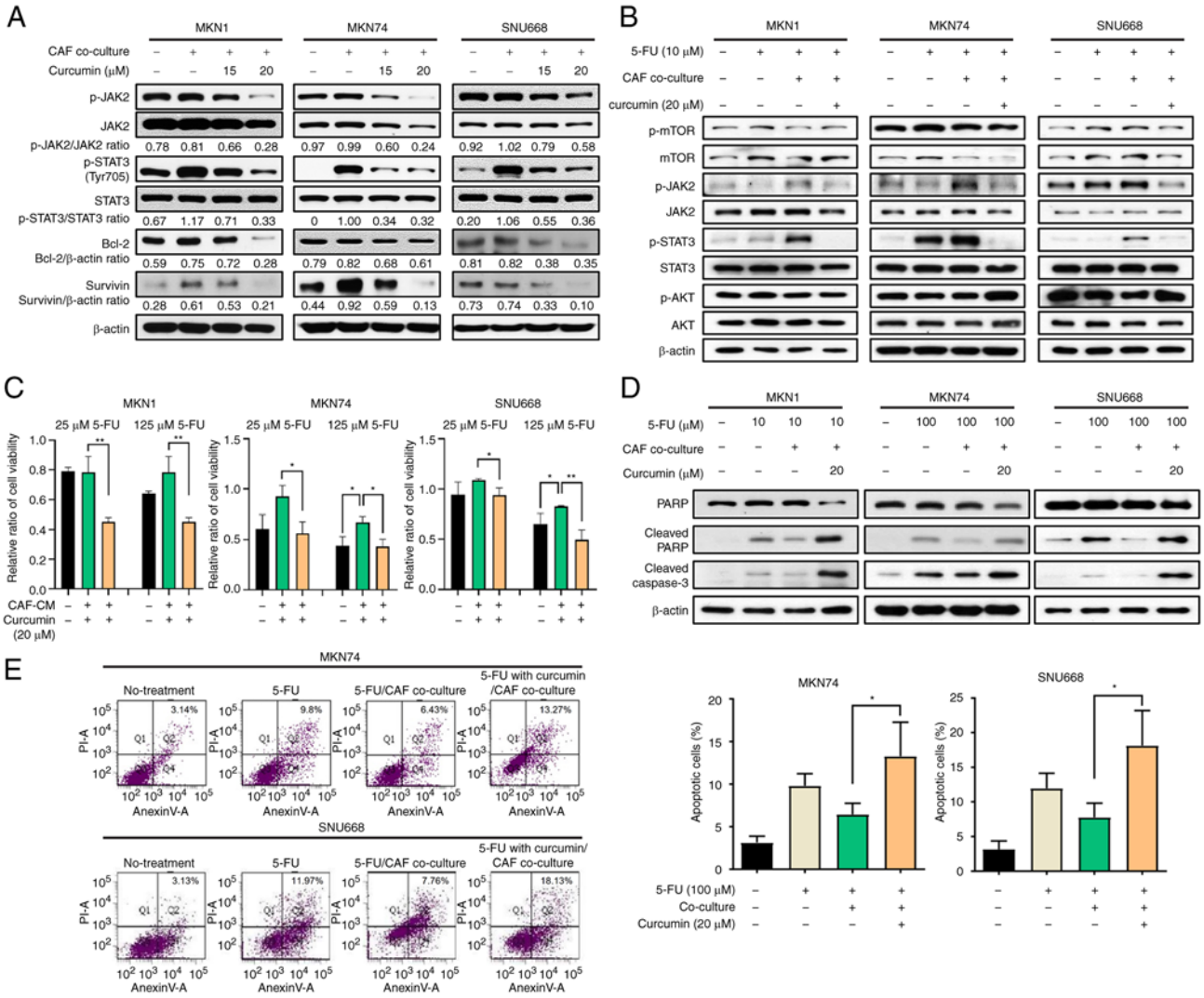

Figure 4. Curcumin inhibits the CAF-induced chemoresistance of GC through the suppression of the JAK/STAT3 signaling pathway. (A) Western blot analysis showing the expression of indicated proteins following co-culture with CAFs and with/without curcumin in MKN1, MKN74 and SNU668 cells. (B) Western blot analysis showing the expression of indicated proteins following co-culture with CAFs and with/without curcumin under 5-FU treatment. (C) Relative viability of MKN74 and SNU668 cells co-cultured with fibroblast culture-conditioned media and treated with 5-FU and curcumin. (D) Western blot analysis showing changes in the expression of apoptotic markers, such as cleaved PARP, at 72 h following 5-FU and curcumin treatment of GC cells with or without co-culture with CAFs. (E) Flow cytometry with Annexin V/PI double-staining showing that 5-FU treatment with curcumin significantly increased the number of Annexin V+/PI+ cells. Data are presented as the mean values. *P<0.05 and **P<0.01. 5-FU, 5-fluorouracil; CAF, cancer-associated fibroblast; JAK, Janus-activated kinase; STAT3, signal transducer and activator of transcription 3.

mTOR and AKT (Fig. S2). Following treatment with 5-FU, the CAF-induced phosphorylation of JAK2/STAT3 was compromised by curcumin treatment in GC cell lines (Fig. 4B).

It was demonstrated that the four types of cytokines (CCL2, CXCL1, IL-6 and IL-8) from the KEGG pathway analysis affected the JAK2/STAT3 signaling pathway in GC cells. Western blot analysis revealed that the levels of p-JAK2/STAT3 increased following treatment with the four cytokines in GC cell lines; however, the expression of mTOR/AKT was not altered. Curcumin decreased the JAK2/STAT3 phosphorylation levels, similar to treatment following co-culture with CAFs (Fig. S3A). These results indicate that CAF-derived cytokines (CCL2, CXCL1, IL-6 and IL-8) can stimulate the activation of the JAK2/STAT3 signaling pathway in GC cell lines and may cause the resistance of GC cell lines to 5-FU. To confirm the primary role of CAF-induced STAT3 activation on chemoresistance, CAF-stimulated GC cells were treated with STAT3 specific inhibitor. The STAT3 inhibitor downregulated the CAF-induced phosphorylation of STAT3 in a concentration-dependent manner (Fig. S3B). The cell viability assay revealed that the resistance to 5-FU increased by CAF-CM was reduced by the STAT3 inhibitor (Fig S3C). Those findings indicated that the curcumin-induced inhibition of phosphorylation of STAT3 could cause the synergistic effect of 5-FU in CAF-stimulated GC cells.

To determine the effects of curcumin on the CAF-induced chemoresistance of GC cell lines, the present study then whether curcumin added to the CAF-CM decreased resistance compared to the cells cultured with CAF-CM and treated only with 5-FU using cell viability assay. The CM from CAF cultures was added to the MKN1, MKN74, and SNU668 cells treated with 5-FU. The cell viability assay revealed that co-treatment with CAF-CM decreased the cytotoxicity of 5-FU. However, treatment with curcumin significantly

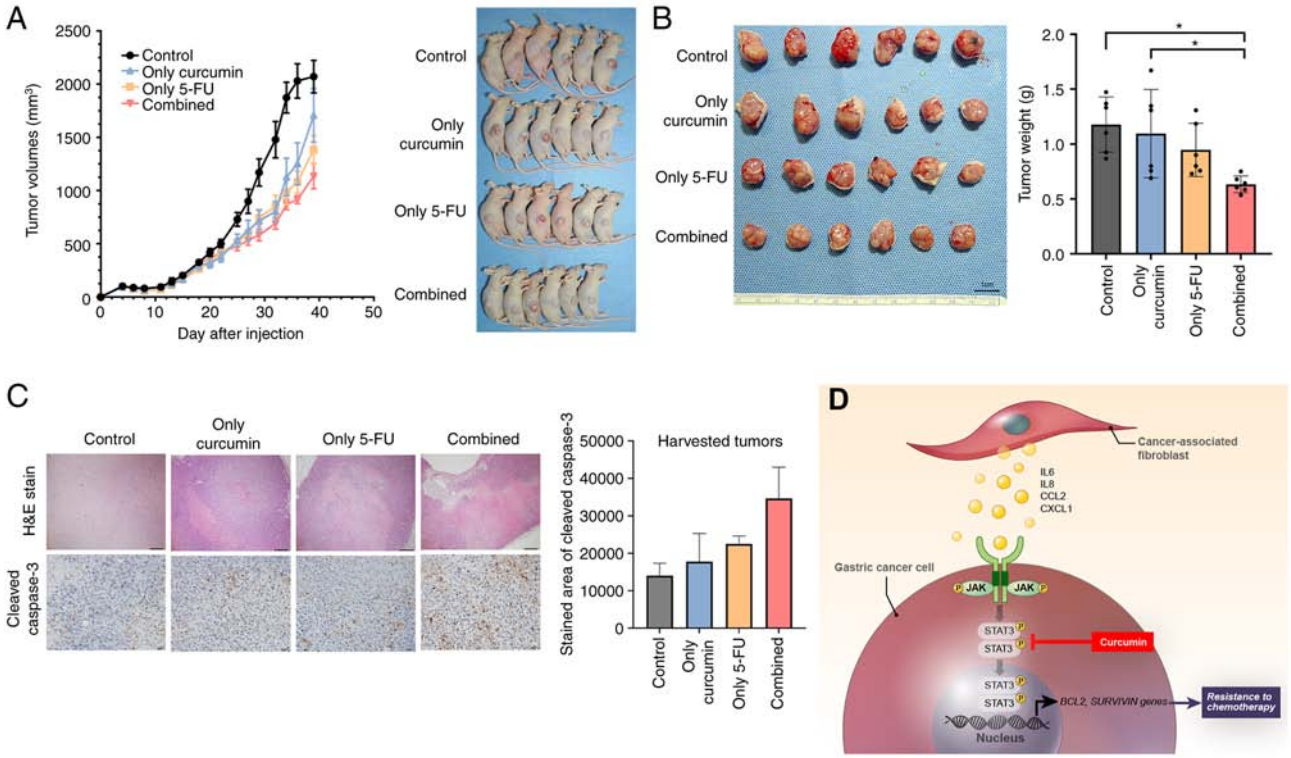

Figure 5. GC xenograft tumor growth inhibition by combination treatment with Curcumin and 5-FU. (A) Mice growing subcutaneous tumors were randomized to receive 21 intraperitoneal injections three times a week of either DMSO or 5-FU or curcumin or combined treatment (5-FU + curcumin). The tumor volume was measured using calipers (n=6 mice in each group) (B) The tumor weight was measured using a precision electronic balance. Representative images of excised tumors in SNU668 models. Scale bar, 1 cm. (C) Representative micrographs showing H&E staining and immunohistochemical staining for cleaved caspase-3 in harvested xenograft tumors derived from SNU668 cells mixed with CAFs after treatment. Scale bar, 100 μm. (D) Schematic diagram of the findings of the present study. CAF-induced cytokines activate the JAK2/STAT3 pathway in gastric cancer cells via paracrine signaling, which allows tumor cells to increasingly oppose apoptosis and increase their survival and resistance to chemotherapy. Curcumin, inhibitor for STAT3, that is a nature product, inhibits the CAF-induced activation of the JAK2/STAT3 signaling pathway in GC cells and consequently enhance the efficacy of chemotherapeutic drugs. 5-FU, 5-fluorouracil; GC, gastric cancer; CCL2, C-C motif chemokine ligand 2; CAF, cancer-associated fibroblast; H&E, hematoxylin and eosin; IL-6, interleukin-6; IL-8, interleukin-8; JAK, Janus-activated kinase; STAT3, signal transducer and activator of transcription 3. *P<0.05.

decreased the viability of the GC cell lines (Fig. 4C). These data strongly suggest that curcumin treatment increased the sensitivity of CAFs to 5-FU in GC cell lines. Moreover, to determine the mechanisms through which curcumin affects the resistance of GC cells treated with 5-FU to apoptosis, the GC cells co-cultured with CAFs were treated with curcumin and 5-FU. The induction of apoptosis was confirmed through cleaved PARP and caspase-3 expression in the GC cell lines. The results revealed that the increased levels of cleaved PARP and caspase-3 upon 5-FU treatment were suppressed by CAF co-culture, and then restored by curcumin treatment (Fig. 4D). Furthermore, under the same conditions, the changes in the proportion of Annexin V and PI double-positive MKN74 and SNU668 cells was monitored using FACS analysis (P<0.05; Fig. 4E). These results suggest that CAFs confer the resistance of GC cell lines to 5-FU through the inhibition of apoptosis, and that curcumin attenuates the chemoresistance of GC cell lines through the JAK2/STAT3 signaling pathway.

Combined treatment with curcumin and 5-FU inhibits CAF-induced tumor growth in the xenograft model of human GC. To investigate whether curcumin contributes to suppressed tumorigenesis in a mouse model, a GC cell line and patient-derived primary CAFs were established using a previously described method (23). In previous research, the authors investigated the *in vivo* effect of fibroblasts on resistance to 5-FU in GC cell line xenografts (8), which were established using only GC cell lines ($1x10^6$ cells each) or mixed with CAFs ($1x10^5$). Tumor volume in xenografts mixed with CAFs suppressed the effects of 5-FU. Therefore, the present study investigated whether combination treatment (curcumin and 5-FU) suppressed the growth of GC cell line-derived xenografts ($1x10^6$ cells each) mixed with CAFs ($5x10^5$). Six mice were used in each group. The results demonstrated that combined treatment suppressed the tumor volume of the xenografts mixed with CAFs (Fig. 5A). The mean weight of the extracted tumors from the mice injected with GC cells mixed with CAFs and subjected to combination treatment (curcumin and 5-FU) was significantly lower than that of the single treatment and control (DMSO). By contrast, the combination treatment was not significantly different from that of the 5-FU treatment alone (Fig. 5B). The diameter of the tumor was 10.75 by 10.47 and the maximum tumor volume in a single treatment group was 589.21 mm^3 according to the calculation method. IHC revealed that the addition of curcumin to the 5-FU treatment of CAF-mixed tumors upregulated the expression of cleaved caspase-3 compared to the vehicle treatment group (Fig. 5C). During treatment, all mice survived and there was no difference in mouse body weight among the treatment groups (Fig. S4). Overall, the *in vivo* experiments revealed

that curcumin treatment increased the sensitivity of xenograft tumors containing CAFs to 5-FU through increased apoptosis without any other side-effects observed in the mice.

Discussion

In the present study, it was found that CAF-produced cytokines, such as IL-6 and IL-8, and chemokines, such as CCL2 enhanced resistance to chemotherapy through the activation of the JAK2/STAT3 axis in GC cells. It was also confirmed that the CAF-activated JAK2/STAT3 axis was efficiently inhibited by the natural product, curcumin. Finally, the present study examined whether curcumin could restore resistance to chemotherapy in the *in vitro* and *in vivo* experimental models (Fig. 5D).

In a previous study by the authors, it was demonstrated that IL-6 usually originates from CAFs in GC tissues and is consequently involved in resistance to chemotherapy through the activation of the JAK/STAT3 signaling pathway in GC cells (8). In addition, it was found that the IL-6 receptor inhibitor exerted a negative effect on CAF-induced resistance in GC experimental models (8). However, CAFs may be a source of other secreted proteins, such as IL-8 or CCL2, which can enhance the JAK/STAT3 pathway (28,29). Thus, the inhibition of the common JAK/STAT3 pathway would be more ideal for reducing the effect of CAFs on GC cells than the IL-6R inhibitor. In the present study, secretome analysis revealed that the levels of IL-6, IL-8 and CCL2 were increased in CAF-co-cultured CM compared to the CM of cancer cells cultured alone. In addition, transcriptome analysis with gene function analysis revealed that the upregulated genes in CAFs co-cultured with GC cells positively correlated with the JAK/STAT3 subset, and this result was validated using western blot analysis. It was hypothesized that CAF-derived molecules may be candidates for activating the JAK/STAT3 signal transduction pathway in GC cells involved in resistance to chemotherapy.

STAT proteins are involved in the regulation of essential signal transduction pathways that control proliferation, differentiation and cell homeostasis (13,30,31). The receptors activated by ligand-binding can phosphorylate specific tyrosine residues of STAT proteins through activation of members of the Janus family of protein tyrosine kinases (JAKs). Of the seven STAT subtypes, STAT3 has been suggested as a critical mediator in maintaining the aggressive phenotype in many cancer cells through its retained activity (32). Moreover, previous studies have reported that the increased phosphorylation of STAT3 is associated with a poor response to chemoradiation, and the inhibition of STAT3 sensitizes cancer cells to 5-FU treatment through the downregulation of STAT3-dependent proteins, such as cyclin D or survivin (33-36). These previous results support the findings of the present study, demonstrating that CAF-induced STAT3 activation promotes resistance to chemotherapy in GCs. Therefore, the suppression of JAK/STAT3 signaling activated by CAFs may be an effective therapeutic strategy to overcome fibrotic stroma-induced resistance to chemotherapy.

Over the past several decades, various strategies have been tested to target STAT3 for the development of potential anticancer drugs. These include small molecules that target different domains of STAT3 and decoy oligonucleotides. The structural analysis of STAT3 has generated several chemicals, such as OPB-31121 or C188-9, targeting the SH2 domain of STAT3, and these have yielded promising results in experimental studies (37,38). However, OPB-31121 in phase I clinical trials for hepatocellular carcinoma only yielded a minimal response, while poor pharmacokinetic properties and severe peripheral nerve toxicity were observed (39). In addition, a number of other chemical drugs targeting STAT3 often exert adverse effects, such as fatigue, infection and diarrhea, which may be related to the physiological function of STAT3 in non-cancerous tissues; thus, few drugs targeting STAT3 have currently been approved for use in clinical settings (40). Curcumin, a natural product derived from turmeric used as a dietary spice and coloring agent, has a negative effect on the binding of JAK protein to cytokine receptors, thereby blocking the phosphorylation and activation of STAT3 (22). It was first tested in an experimental model of lung cancer, demonstrating an inhibitory effect on STAT3 phosphorylation in a time-and concentration-dependent manner (22). In addition, curcumin inhibits IL-6 induced STAT3 phosphorylation in myeloma cells (41). While the drug metabolites generated from synthetic drug sources can create a variety of adverse side-effects, drugs formed from natural sources, such as curcumin, may have limited side-effects. In the present study, low concentrations of curcumin, which was not toxic to GC cells, effectively suppressed CAF-induced JAK/STAT3 activation, as well as STAT3-dependent proteins, such as Bcl-2 and survivin. Moreover, additional low-dose curcumin had a positive effect on chemotherapy-induced apoptosis in experimental models. These results suggest that low-dose curcumin treatment or a turmeric-based diet during chemotherapy in GC patients may be an effective strategy which may be used to improve the response.

In the present study, in the animal experiments, although additional curcumin treatment significantly reduced tumor growth compared to the control, it did not exhibit a significant difference from the 5-FU treatment alone. In fact, the limitation of curcumin is its low bioavailability and short time for metabolization as a natural product. Therefore, different curcumin analogs have been synthesized to increase their stability. FLLL32 has two hydrogens of curcumin replaced with a spiro-cyclohexyl ring and methyl groups, which can improve its stability (42). Several previous reports have described that FLLL32 potently reduced tumor growth of xenografts in bone and breast cancers (43,44). Therefore, curcumin analogs more effectively improve the response to chemotherapy in GC models, including CAFs, compared to curcumin, in future studies.

In conclusion, the present study demonstrated that CAFs enhanced resistance to chemotherapy in GC through the activation of the JAK2/STAT3 signaling pathway. Curcumin, a natural product derived from turmeric, effectively reduced CAF-induced STAT3 activation in GC cells and subsequently enhanced the effects of chemotherapy in GC models. The combination of curcumin and conventional chemotherapy may thus be a promising strategy with which to overcome resistance to chemotherapy in GC with profuse fibroblasts.

Acknowledgements

Not applicable.

Funding

The present study was supported by grants from the National Research Foundation of Korea (NRF) funded by the Ministry of Education (no. 2020R1A6A1A03043539 and 2020R1I1A1A01070961 and a NRF grant funded by the Korean government, the Ministry of Science and ICT (no. 2020R1A2C1006273).

Availability of data and materials

The datasets used and/or analyzed during the current study are available from the corresponding author on reasonable request.

Authors' contributions

IHH and HH performed the majority of the experiments, analyzed the data and managed the clinical information, and were also involved in the conception and design of the study. LW and HH provided the resources. DL, KSC, HJO and THK were involved in data curation. LW, HYJ, and TMK were involved in formal analysis. JW and IHH were involved in the investigative aspects of the study (e.g., data collection). JW, IHH and HH drafted the manuscript. IHH, HH and HJO provided administrative, technical, or material support. IHH, KSC and HH supervised the study. IHH and HH confirm the authenticity of all the raw data. All authors have read and approved the final manuscript.

Ethics approval and consent to participate

The present study was approved by the Ethics Committee of Shanghai Cancer Center (IRB No. 050432-4-1911D). Informed consent was obtained from all the participants, and procedures were conducted according to the Declaration of Helsinki. Animal care and handling procedures were performed in accordance with the Ajou University School of Medicine Institution Animal Care and Use Committee guidelines, and all animal experiments were approved by the Animal Research Committee of the institution.

Patient consent for publication

Not applicable.

Competing interests

The authors declare that they have no competing interests.

References

1. Bray F, Ferlay J, Soerjomataram I, Siegel RL, Torre LA and Jemal A: Global cancer statistics 2018: GLOBOCAN estimates of incidence and mortality worldwide for 36 cancers in 185 countries. CA Cancer J Clin 68: 394-424, 2018.
2. Wagner AD, Grothe W, Haerting J, Kleber G, Grothey A and Fleig WE: Chemotherapy in advanced gastric cancer: A systematic review and meta-analysis based on aggregate data. J Clin Oncol 24: 2903-2909, 2006.
3. Guideline Committee of the Korean Gastric Cancer Association (KGCA), Development Working Group & Review Panel: Korean practice guideline for gastric cancer 2018: An evidence-based, multi-disciplinary approach. J Gastric Cancer 19: 1-48, 2019.
4. Japanese Gastric Cancer Association: Japanese gastric cancer treatment guidelines 2018 (5th edition). Gastric Cancer 24: 1-21, 2021.
5. Wu Y, Grabsch H, Ivanova T, Tan IB, Murray J, Ooi CH, Wright AI, West NP, Hutchins GG, Wu J, *et al*: Comprehensive genomic meta-analysis identifies intra-tumoural stroma as a predictor of survival in patients with gastric cancer. Gut 62: 1100-1111, 2013.
6. Lei Z, Tan IB, Das K, Deng N, Zouridis H, Pattison S, Chua C, Feng Z, Guan YK, Ooi CH, *et al*: Identification of molecular subtypes of gastric cancer with different responses to PI3-kinase inhibitors and 5-fluorouracil. Gastroenterology 145: 554-565, 2013.
7. Ma J, Song X, Xu X and Mou Y: Cancer-associated fibroblasts promote the chemo-resistance in gastric cancer through secreting IL-11 targeting JAK/STAT3/Bcl2 pathway. Cancer Res Treat 51: 194-210, 2019.
8. Ham IH, Oh HJ, Jin H, Bae CA, Jeon SM, Choi KS, Son SY, Han SU, Brekken RA, Lee D and Hur H: Targeting interleukin-6 as a strategy to overcome stroma-induced resistance to chemotherapy in gastric cancer. Mol Cancer 18: 68, 2019.
9. Kalluri R: The biology and function of fibroblasts in cancer. Nat Rev Cancer 16: 582-598, 2016.
10. Kalluri R and Zeisberg M: Fibroblasts in cancer. Nat Rev Cancer 6: 392-401, 2006.
11. Kuzet SE and Gaggioli C: Fibroblast activation in cancer: When seed fertilizes soil. Cell Tissue Res 365: 607-619, 2016.
12. Resemann HK, Watson CJ and Lloyd-Lewis B: The Stat3 paradox: A killer and an oncogene. Mol Cell Endocrinol 382: 603-611, 2014.
13. Aaronson DS and Horvath CM: A road map for those who don't know JAK-STAT. Science 296: 1653-1655, 2002.
14. Sweet K, Hazlehurst L, Sahakian E, Powers J, Nodzon L, Kayali F, Hyland K, Nelson A and Pinilla-Ibarz J: A phase I clinical trial of ruxolitinib in combination with nilotinib in chronic myeloid leukemia patients with molecular evidence of disease. Leuk Res 74: 89-96, 2018.
15. McLornan DP, Khan AA and Harrison CN: Immunological consequences of JAK inhibition: Friend or foe? Curr Hematol Malig Rep 10: 370-379, 2015.
16. Wake MS and Watson CJ: STAT3 the oncogene-still eluding therapy? FEBS J 282: 2600-2611, 2015.
17. Gupta SC, Patchva S, Koh W and Aggarwal BB: Discovery of curcumin, a component of golden spice, and its miraculous biological activities. Clin Exp Pharmacol Physiol 39: 283-299, 2012.
18. Lee WH, Bebawy M, Loo CY, Luk F, Mason RS and Rohanizadeh R: Fabrication of curcumin micellar nanoparticles with enhanced anti-cancer activity. J Biomed Nanotechnol 11: 1093-1105, 2015.
19. Lee WH, Loo CY, Young PM, Rohanizadeh R and Traini D: Curcumin nanoparticles attenuate production of pro-inflammatory markers in lipopolysaccharide-induced macrophages. Pharm Res 33: 315-327, 2016.
20. Lee WH, Loo CY, Young PM, Traini D, Mason RS and Rohanizadeh R: Recent advances in curcumin nanoformulation for cancer therapy. Expert Opin Drug Deliv 11: 1183-1201, 2014.
21. Wong TF, Takeda T, Li B, Tsuiji K, Kitamura M, Kondo A and Yaegashi N: Curcumin disrupts uterine leiomyosarcoma cells through AKT-mTOR pathway inhibition. Gynecol Oncol 122: 141-148, 2011.
22. Byun SY, Kim DB and Kim E: Curcumin ameliorates the tumor-enhancing effects of a high-protein diet in an azoxymethane-induced mouse model of colon carcinogenesis. Nutr Res 35: 726-735, 2015.
23. Yang CL, Liu YY, Ma YG, Xue YX, Liu DG, Ren Y, Liu XB, Li Y and Li Z: Curcumin blocks small cell lung cancer cells migration, invasion, angiogenesis, cell cycle and neoplasia through Janus kinase-STAT3 signalling pathway. PLoS One 7: e37960, 2012.
24. Lee D, Ham IH, Son SY, Han SU, Kim YB and Hur H: Intratumor stromal proportion predicts aggressive phenotype of gastric signet ring cell carcinomas. Gastric Cancer 20: 591-601, 2017.
25. Ryan R, Gibbons D, Hyland JM, Treanor D, White A, Mulcahy HE, O'Donoghue DP, Moriarty M, Fennelly D and Sheahan K: Pathological response following long-course neoadjuvant chemoradiotherapy for locally advanced rectal cancer. Histopathology 47: 141-146, 2005.

26. Cristescu R, Lee J, Nebozhyn M, Kim KM, Ting JC, Wong SS, Liu J, Yue YG, Wang J, Yu K, *et al*: Molecular analysis of gastric cancer identifies subtypes associated with distinct clinical outcomes. Nat Med 21: 449-456, 2015.
27. Wang H, Wu X and Chen Y: Stromal-immune score-based gene signature: A prognosis stratification tool in gastric cancer. Front Oncol 9: 1212, 2019.
28. Tsuyada A, Chow A, Wu J, Somlo G, Chu P, Loera S, Luu T, Li AX, Wu X, Ye W, *et al*: CCL2 mediates cross-talk between cancer cells and stromal fibroblasts that regulates breast cancer stem cells. Cancer Res 72: 2768-2779, 2012.
29. Wu J, Gao FX, Wang C, Qin M, Han F, Xu T, Hu Z, Long Y, He XM, Deng X, *et al*: IL-6 and IL-8 secreted by tumour cells impair the function of NK cells via the STAT3 pathway in oesophageal squamous cell carcinoma. J Exp Clin Cancer Res 38: 321, 2019.
30. O'Shea JJ, Holland SM and Staudt LM: JAKs and STATs in immunity, immunodeficiency, and cancer. N Engl J Med 368: 161-170, 2013.
31. Quintás-Cardama A and Verstovsek S: Molecular pathways: Jak/STAT pathway: Mutations, inhibitors, and resistance. Clin Cancer Res 19: 1933-1940, 2013.
32. Birner P, Toumangelova-Uzeir K, Natchev S and Guentchev M: STAT3 tyrosine phosphorylation influences survival in glioblastoma. J Neurooncol 100: 339-343, 2010.
33. Qin A, Yu Q, Gao Y, Tan J, Huang H, Qiao Z and Qian W: Inhibition of STAT3/cyclinD1 pathway promotes chemotherapeutic sensitivity of colorectal caner. Biochem Biophys Res Commun 457: 681-687, 2015.
34. Spitzner M, Roesler B, Bielfeld C, Emons G, Gaedcke J, Wolff HA, Rave-Fränk M, Kramer F, Beissbarth T, Kitz J, *et al*: STAT3 inhibition sensitizes colorectal cancer to chemoradiotherapy in vitro and in vivo. Int J Cancer 134: 997-1007, 2014.
35. Stella S, Tirrò E, Conte E, Stagno F, Di Raimondo F, Manzella L and Vigneri P: Suppression of survivin induced by a BCR-ABL/JAK2/STAT3 pathway sensitizes imatinib-resistant CML cells to different cytotoxic drugs. Mol Cancer Ther 12: 1085-1098, 2013.
36. Wen K, Fu Z, Wu X, Feng J, Chen W and Qian J: Oct-4 is required for an antiapoptotic behavior of chemoresistant colorectal cancer cells enriched for cancer stem cells: Effects associated with STAT3/survivin. Cancer Lett 333: 56-65, 2013.
37. Brambilla L, Genini D, Laurini E, Merulla J, Perez L, Fermeglia M, Carbone GM, Pricl S and Catapano CV: Hitting the right spot: Mechanism of action of OPB-31121, a novel and potent inhibitor of the signal transducer and activator of transcription 3 (STAT3). Mol Oncol 9: 1194-1206, 2015.
38. Redell MS, Ruiz MJ, Alonzo TA, Gerbing RB and Tweardy DJ: Stat3 signaling in acute myeloid leukemia: Ligand-dependent and -independent activation and induction of apoptosis by a novel small-molecule Stat3 inhibitor. Blood 117: 5701-5709, 2011.
39. Okusaka T, Ueno H, Ikeda M, Mitsunaga S, Ozaka M, Ishii H, Yokosuka O, Ooka Y, Yoshimoto R, Yanagihara Y and Okita K: Phase 1 and pharmacological trial of OPB-31121, a signal transducer and activator of transcription-3 inhibitor, in patients with advanced hepatocellular carcinoma. Hepatol Res 45: 1283-1291, 2015.
40. Beebe JD, Liu JY and Zhang JT: Two decades of research in discovery of anticancer drugs targeting STAT3, how close are we? Pharmacol Ther 191: 74-91, 2018.
41. Kunnumakkara AB, Anand P and Aggarwal BB: Curcumin inhibits proliferation, invasion, angiogenesis and metastasis of different cancers through interaction with multiple cell signaling proteins. Cancer Lett 269: 199-225, 2008.
42. Bill MA, Fuchs JR, Li C, Yui J, Bakan C, Benson DM Jr, Schwartz EB, Abdelhamid D, Lin J, Hoyt DG, *et al*: The small molecule curcumin analog FLLL32 induces apoptosis in melanoma cells via STAT3 inhibition and retains the cellular response to cytokines with anti-tumor activity. Mol Cancer 9: 165, 2010.
43. Onimoe GI, Liu A, Lin L, Wei CC, Schwartz EB, Bhasin D, Li C, Fuchs JR, Li PK, Houghton P, *et al*: Small molecules, LLL12 and FLLL32, inhibit STAT3 and exhibit potent growth suppressive activity in osteosarcoma cells and tumor growth in mice. Invest New Drugs 30: 916-926, 2012.
44. Yan J, Wang Q, Zou K, Wang L, Schwartz EB, Fuchs JR, Zheng Z and Wu J: Inhibition of the JAK2/STAT3 signaling pathway exerts a therapeutic effect on osteosarcoma. Mol Med Rep 12: 498-502, 2015.